ShahidChamran University of Ahvaz

Iranian Association of Electrical and Electronics Engineers

Journal of Applied Research in Electrical Engineering

E-ISSN: 2783-2864
P-ISSN: 2717-414X
Homepage:https://jaree.scu.ac.ir/

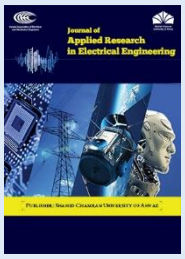

Research Article

A New Approach for the Transformer Differential Protection Based on S-Transform and Fuzzy Expert System

Saeid Hasheminejad*

Department of Electrical and Computer Engineering, Graduate University of Advanced Technology, Kerman, Iran.

**Corresponding Author: SaeidHasheminejad@yahoo.com*

Abstract: This paper presents a novel method to discriminate between the magnetizing inrush and external and internal fault currents in power transformers. Fault type identification and faulted phase selection are also possible by the proposed algorithm. The proposed method has two main parts. First, by means of S-transform, which is the most accurate method in the field of signal processing, some useful features are extracted from the input signal. Then, the extracted features are converted to some numerical indices. In the second part, an effective decision maker is needed to classify the input signal. One of the best methods, which have been used for decision-making applications is fuzzy logic. So, the numerical indices are used as inputs for the fuzzy system. The output of the fuzzy system not only can reveal whether the input signal is the magnetizing inrush, external or internal fault, but it can also identify the fault type when there is an internal fault. Finally, the faulted phases can be identified with a supplemental algorithm. To generate the test signals, a three-phase transformer is modeled in PSCAD/EMTDC. Testing the proposed algorithm by different simulated data shows the robustness of the proposed method in the transformer differential protection.

Keywords: Transformer differential protection, inrush current, internal fault, S-transform, fuzzy expert system.

Article history
Received 01 September 2021; Revised 31 December 2021; Accepted 31 December 2021 Published online 9 March 2022.

How to cite this article
S. Hasheminejad, "A new approach for the transformer differential protection based on S-transform and fuzzy expert system," *J. Appl. Res. Electr. Eng.*, vol. 1, no. 2, pp. 159-168, 2022. DOI: 10.22055/jaree.2021.38432.1035

Check for updates

1. INTRODUCTION

Power transformers are considered as one of the most important components of a power system. The protection of different components of a power system is also a critical issue. Therefore, fast and reliable protection of the power transformers is an important problem that needs to be addressed properly. The accurate protection of these transformers can decrease possible damages and increase the reliability of the power supply. There are some special operating conditions that can lead to the reduction of the protection accuracy [1]. It can be said that there are some disturbances, such as magnetizing inrush, internal fault, external fault, and ultra-saturation, which can affect the performance of a power transformer [2-3]. The protection scheme for a transformer must be reliable (no missing operation), secure (no false tripping), fast (short fault clearing time), and stable [4].

When an internal fault occurs, the protection relay should be able to trip the transformer from the network to limit the internal damage caused by the fault to the transformer. Differential relaying plays the main role in the electrical protection of a power transformer. When there is an internal fault, a differential current flow through the relay whose amplitude is much higher than the differential current amplitude in the normal operating condition. This quantity can be used as a discriminative feature to understand a fault condition. But, in some situations, differential current can have a high value, and relay should not perform. In fact, when a transformer is energized, a magnetizing inrush current will flow through the transformer and cause the differential current to have a high value. It is a transient current that does not damage the transformer, so there is no need to trip the transformer. The same condition occurs when the transformer is energized in parallel with an already operating transformer [5] or when the transformer recovers from an external fault. The external fault can also make the amplitude of the

differential current much higher than its usual value but it should not make the differential relay trip the transformer.

Taking all the above into consideration, it can be understood that a protective scheme must be able to distinguish internal faults from inrush currents and external faults. Magnetizing inrush currents have a high level of the second harmonic component that was traditionally a discriminative feature to distinguish the magnetizing inrush currents from the internal faults [6], [7]. Methods that are based on the second harmonic component are no longer applicable in the transformer differential protection because there are some contents of the second harmonic component, while CT saturates. Moreover, there can be a low level of the second harmonic component in the magnetizing inrush currents due to the modern core material of the power transformer [8], [9]. There are other methods that are based on the waveform identification. In these methods, some features are extracted from the signal waveform and according to these features, it is decided if the waveform is an internal fault or a magnetizing inrush current [10].

Various methods have recently been presented to solve this problem. Some have used artificial neural networks and genetic algorithms to identify the inrush current [11, 12], which are system-dependent and impose a high computational burden. Others have used wavelet transform (WT) for this purpose [13-14]. WT can be affected by the high-frequency noise, which is a considerable drawback [15]. Other drawback of utilizing WT is the dependability of its accuracy on the choice of the mother wavelet, which can only be derived by trial and error. In [16], an algorithm that is based on the wave shape properties of the transformer average differential power during inrush and internal faults is used to discriminate between these two events. A method based on the Clarke transform with fuzzy sets is presented in [17], and methods based on the wavelet pocket transform are presented in [18] and [19] to be used for the differential protection of the power transformers. A Kalman-filter-based algorithm is presented in [20] for the same purpose.

Another phenomenon that leads to an over-current in the transformer differential relays is the external fault, which has not been considered in the above-reviewed papers. Since the external faults are not related to any faults in the transformer, the differential relay should not operate in this situation. This paper presents an effective method based on the S-transform and fuzzy system. The proposed method can discriminate between the internal faults, external faults, and inrush currents. This method is based on the characteristics derived from the wave shapes of these three signal types. S-transform is a convertible time-frequency analyzing technique and has not only the useful characteristics of both Fourier transform (FT) and wavelet transform (WT) but also characteristics superior to both previous time-frequency analyzing techniques. FT cannot extract non-stationary features of the signals, so it is not possible to use it to analyze the transient signals such as the magnetizing inrush currents. As mentioned before, high-frequency noise and the choice of the mother wavelet affect the accuracy of WT. S-transform can extract both the time and frequency properties of the signals. As a result, it can be used to extract transient information of the signals. This method is immune to noise and there is no need for any mother wavelet or things like that [21].

After the feature extraction, an effective classifier is needed to classify the input signals. In this paper, a fuzzy system is used to classify the input signals to reveal if there is an internal fault, an external fault, or a magnetizing inrush. In addition, when there is an internal fault, the proposed method can extract the fault type, whether there is a single-phase, double-phase, double-phase-to-ground, three-phase, or three-phase-to-ground fault. The phases that have encountered a fault will be revealed then.

2. Power Transformer Specifications

For the simulation purpose, a three-phase transformer is simulated in PSCAD/EMTDC software. Different signals are extracted from the simulated transformer.

2.1. Magnetic Core Saturation

The magnetic core saturation is simulated by compensating for the current source across the winding wound closest to the core [22]. The simulation model is shown in Fig. 1.

In Fig. 1, $I_s(t)$ is the magnetizing current that is related to the flux linkage through the $\lambda - I$ characteristic and can be derived from the voltage and current measurements during the no-load test. In the case of having a high value for the linkage flux, the slope of this curve tends toward the saturated core inductance of the transformer winding. This characteristic is calculated by means of the PSCAD/EMTDC platform based on the magnetizing current at the rated voltage, the air core saturated reactance of the winding and the position of the knee point.

2.2. Remanence

When a transformer works in its normal operation, the flux linkages corresponding to the three phases have the same magnitude with 120° phase deviation. In the case of de-energizing the transformer, the linkage flux will freeze at the flux remanence point. The degree of the magnetizing inrush current during energization is a direct function of the remanence that exists in the leg of the transformer core. So, it is necessary to simulate the residual flux of the core. Residual flux can be simulated by inserting a controlled DC current source in parallel to each low-voltage transformer winding [23].

2.3. Inrush Current

The existence of the inrush current in a power transformer has different reasons. It is mostly the result of the transformer energization. Recovering the transformer from an external fault and energizing the transformer in parallel to an already operated transformer are other reasons for the existence of an

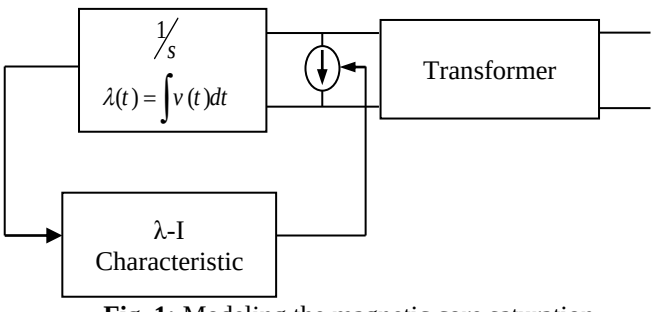

Fig. 1: Modeling the magnetic core saturation.

inrush current for the existence of an inrush current in a power transformer. Inrush currents are transient currents that flow through the transformer windings for several cycles and their initial amplitude is much higher than the transformer's nominal current. A magnetizing inrush current has the following features:

- It consists of the DC offset and odd and even harmonics (especially the second harmonic component).
- There are uni-polar or bi-polar pulses along with low current value intervals.
- The ratio of the second harmonic component to the first one has a relatively high value.

There are time intervals between pulses with very low current values [24].

2.4. Internal Fault

Internal faults are the other reason for having high amplitude differential currents in the transformer windings. The common features of the internal fault currents are as follows**:**

- There is a DC offset in some of the internal fault currents.
- In the first moments after the fault inception, the slope of the internal fault current is higher than that of the inrush current.
- If there is no harmonic in the system, the internal fault has a sinusoidal trend.

The following items have a considerable effect on the internal fault current specifications:

- Fault type (single-phase-to-ground (SLG), double-phase-to-ground (DLG), double-phase (LL) and three-phase (3PH)).
- Load condition
- The phase voltage at the instant of the fault inception
- The impedance of the fault.

2.5. External fault

Sometimes when an external fault occurs, a relatively high magnitude current flows through the differential relay. For example, in the case of the CT saturation, external faults lead to the high amplitude differential currents. The fault type, fault inception angle, fault impedance and the transformer core remanence flux are some of the main parameters that affect the external fault specifications.

3. S TRANSFORM

The S transform (ST), introduced by Stockwell [25], can be considered the "phase correction" of the continuous wavelet transform (CWT). The CWT of the function h(t) is defined by:

$$W(\tau,d)=\int_{-\infty}^{\infty} h(t).w(d,t-\tau)dt \tag{1}$$

The ST is a CWT with a specific mother wavelet multiplied by a phase-corrected factor:

$$s(\tau,f)=e^{j2\pi f\tau}.W(d,\tau) \tag{2}$$

where the mother wavelet w(f,t) is defined as:

$$w(f,t)=\frac{|f|}{\sqrt{2\pi}}e^{-\frac{t^2f^2}{2}}.e^{-j2\pi ft} \tag{3}$$

In (1), parameter d is the inverse of the frequency and f is the frequency. Finally, the ST equation can be written as follows:

$$S(\tau,f)=\frac{|f|}{\sqrt{2\pi}}\int_{-\infty}^{\infty} h(t)e^{-\frac{(t-\tau)^2f^2}{2}}e^{-j2\pi ft}dt \tag{4}$$

The ST can also be written as an operation on the Fourier spectrum H(f) of h(t):

$$S(\tau,f)=\int_{-\infty}^{\infty} H(\alpha+f)e^{-\frac{2\pi^2\alpha^2}{f^2}}e^{j2\pi\alpha t}d\alpha \tag{5}$$

Since ST is a representation of the local spectra, Fourier or time average spectrum can be directly calculated by averaging the local spectrum as:

$$H(f)=\int_{-\infty}^{\infty} S(f,\tau)d\tau \tag{6}$$

$$h(t)=\int_{-\infty}^{\infty}\left\{\int_{-\infty}^{\infty} S(f,\tau)d\tau\right\}e^{j2\pi ft}df \tag{7}$$

The power disturbance signal h(t) can be defined in a discrete form as h(kT), k=0, 1, ..., N-1, where T is the sampling time interval and N is the total sampling number. The discrete Fourier transform can be calculated as:

$$H\left[\frac{n}{NT}\right]=\frac{1}{N}\sum_{k=1}^{N-1} h(kT)e^{(-j\frac{2\pi nk}{N})} \tag{8}$$

$$n=0,1,2,...,N-1$$

Using (5), the ST of a discrete time series h(kT) is given by (let $\tau\to kT$ and f $\to$ n/NT)

$$S\left[kT,\frac{n}{kT}\right]=\sum_{m=0}^{n-1} H\left[\frac{m+n}{NT}\right]e^{-\frac{2\pi^2m^2}{n^2}}.e^{j\frac{2\pi mk}{N}}\ 1\ n\neq 0 \tag{9}$$

k,m = 0,1,2,…,N-1 n = 1,2,…,N-1

$$S\left[kT,0\right]=\frac{1}{N}\times\sum_{m=0}^{N-1} h(\frac{m}{NT})\ \ \text{n = 0} \tag{10}$$

So, the ST matrix S [KT, n/KT] is used to analyze the power system signals in which the rows are frequencies and the columns are the time values. Each column displays the ST magnitude with all frequencies at the same time and each row displays the ST magnitude with the time varying from 0 to N-1 in the same frequency where n=0, 1, …, $\frac{N}{2}-1$. In this paper, the ST amplitude (STA) matrix is:

$$A(kT,f)=\left|S\left[kT,\frac{n}{NT}\right]\right| \tag{11}$$

Apart from having the ST amplitude matrix, considering the ST phase matrix (STP) is also profitable to analyze the power quality disturbances in a three-phase manner.

$$P(kT,f)=\arctan\left(\frac{\mathrm{Im}S\left(\left[kT,\frac{n}{NT}\right]\right)}{\mathrm{Re}S\left(\left[kT,\frac{n}{NT}\right]\right)}\right) \tag{12}$$

4. POWER TRANSFORMER DIFFERENTIAL PROTECTION

The algorithm, proposed in this paper, consists of two different steps. In the first step, some features are extracted from the relay signal using a proper time-frequency analyzing technique. In the second step, the relay signal should be classified using a proper classifier according to the features extracted in the previous step.

4.1. Feature Extraction

One of the best methods, which is used for this purpose, is the ST. This technique can be used to extract all frequency, time, and transient features of the signal. Besides, this technique is immune to noise and its output is easy to analyze. The ST output is a complex matrix. If we calculate the absolute value of each component of this matrix, according to (11), we would have an STA matrix that is used for feature extraction. Fig. 2(a) shows the normal signal without any disturbances and Figs. 2(b) and 2(c) are the time-frequency amplitude curves generated from its STA matrix. Here, the sampling frequency is 10 kHz and the signal's main frequency is 50Hz. Fig. 2(b) is called the maximum amplitude curve (MAC), which indicates the frequency components of the input signal. It is extracted from each column of the STA matrix. Fig. 2(c) is called the standard deviation curve (SDC). To explain this curve, the STA matrix should be explained more precisely. When the input signal has n samples, the STA matrix will have n/2 rows and n columns. Each row shows the input signal amplitude deviations versus time, and each column shows the frequency components of the input signal in each time sample. When the input signal has a fixed amplitude, the values in each row of the STA matrix will remain approximately constant. Therefore, the standard deviation of the values of each row is near zero. But, when there is a transient signal added to the main signal, the standard deviation of the respective row (respective frequency which is the frequency of the transient signal) will have a nonzero value. In this paper, we use this curve to detect the fault-generated transient components.

Figs. 3-12 present the sampling signals of the internal fault, inrush current and external fault along with their related three-phase MACs and SDCs. To generate MACs and SDCs, one cycle of each of the three phases is recorded and then ST is applied to the recorded signals. The differential currents are extracted from a Y/Δ, 50Hz, 500 MVA, and 400/230 kV three-phase transformer, which is modeled in PSCAD/EMTDC. Fig. 3 shows the three-phase differential currents related to a Bg fault with 10 Ohms fault resistance and the fault inception angle of 90 degrees. It is worth mentioning that each of Figs. 4, 6, 8, 10, and 12 contains the MACs and SDCs of all the three phases. In fact, samples 1 to 100 are related to phase A, samples 101 to 200 are related to phase B, and samples 201 to 300 are related to phase C.

In Fig. 4, it is expected that the region related to phase B has a peak in both MAC and SDC. For example, in Fig. 4(a), the region related to phase B is between samples 100 and 200. A peak at the beginning of the phase B region shows that there is a peak in the fundamental frequency in the MAC of phase B. Fig. 5 shows an ACg fault with zero Ohms resistance with the fault inception angle of 45 degrees. Note that this angle is the angle of phase A voltage at the fault inception time.

Fig. 7 shows the three-phase currents for a three-phase fault with 5 Ohms resistance with the fault inception angle of 30 degrees.

Fig. 9 shows the three-phase current signals for an inrush situation. Here, the source impedance is 10 Ohms and the voltage angle of phase A is 90 degrees at the switching inception time.

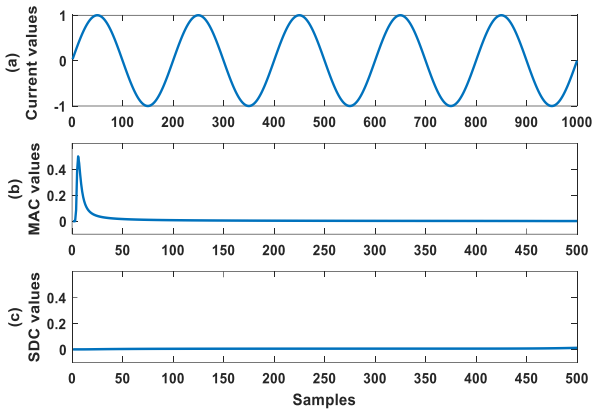

Fig. 2: Normal signal and the related curves extracted by S-transform, (a): Normal signal, (b) MAC values, (c) SDC values.

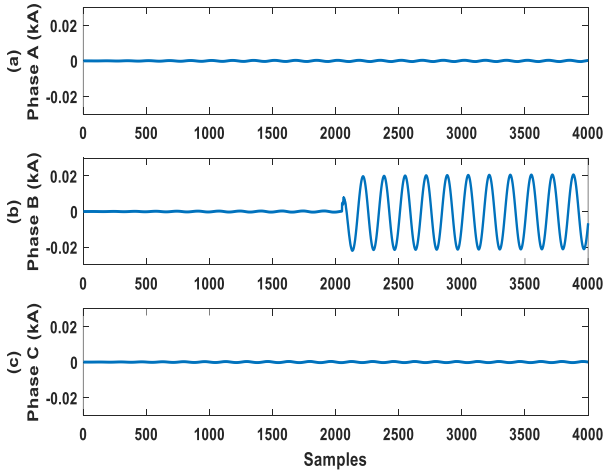

Fig. 3: Differential currents related to a Bg fault, (a) Phase A, (b) Phase B, (c) Phase C.

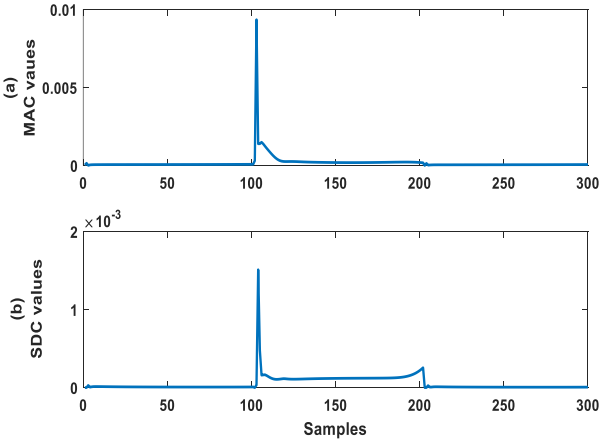

Fig. 4: ST outputs for the three phases for a Bg fault, (a) MAC, (b) SDC.

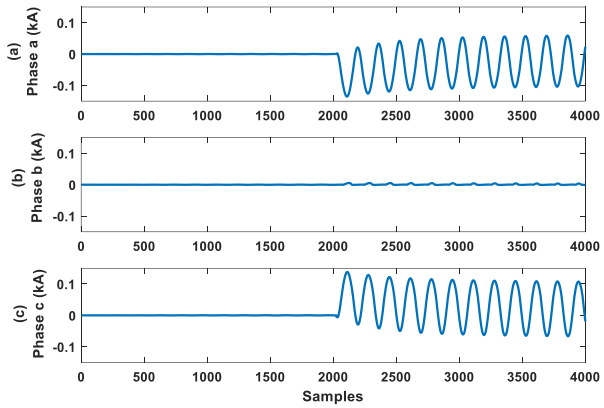

Fig. 5: Sampling data for a double-phase-to-ground fault, (a) Phase A, (b) Phase B, (c) Phase C.

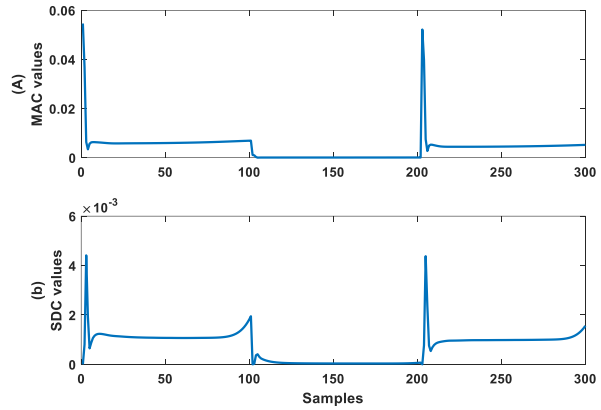

Fig. 6: ST outputs for the three phases for the ACg fault, (a) MAC, (b) SDC.

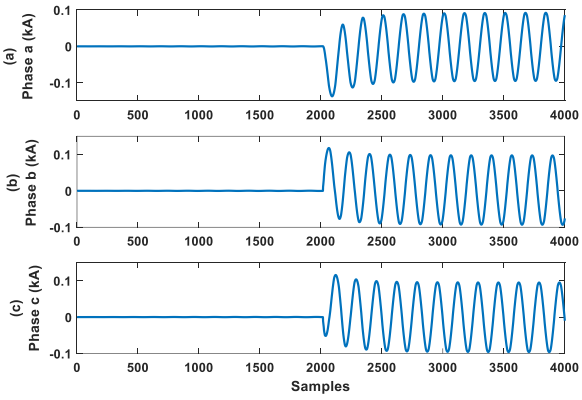

Fig. 7: Sampling data for a three-phase-to-ground fault, (a) Phase A, (b) Phase B, (c) Phase C.

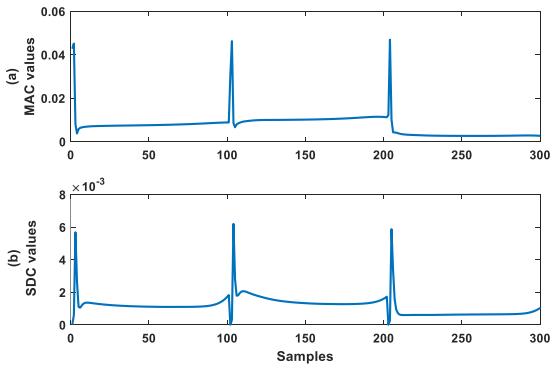

Fig. 8: ST outputs for the three phases for the ABC fault, (a) MAC, (b) SDC.

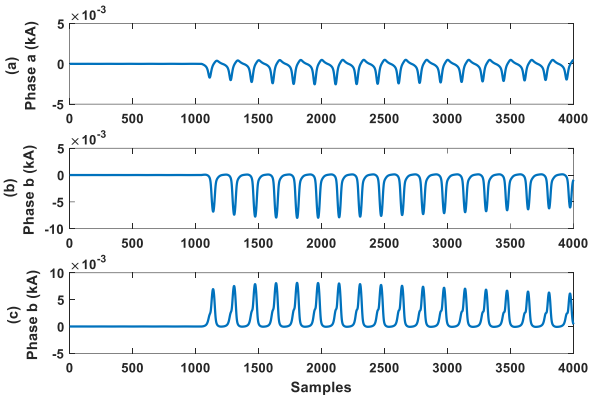

Fig. 9: Sampling data for an inrush current, (a) Phase A, (b) Phase B, (c) Phase C.

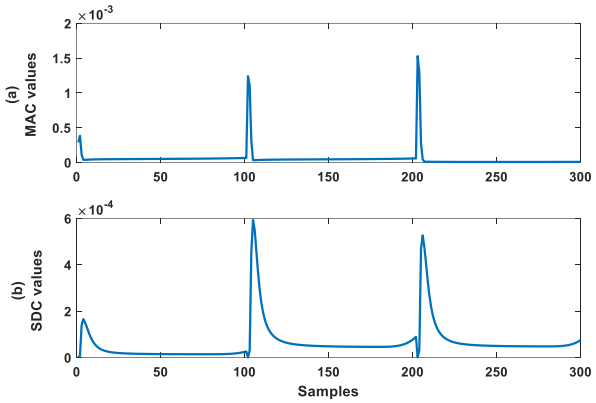

Fig. 10: ST outputs for the three phases for an inrush current, (a) MAC, (b) SDC.

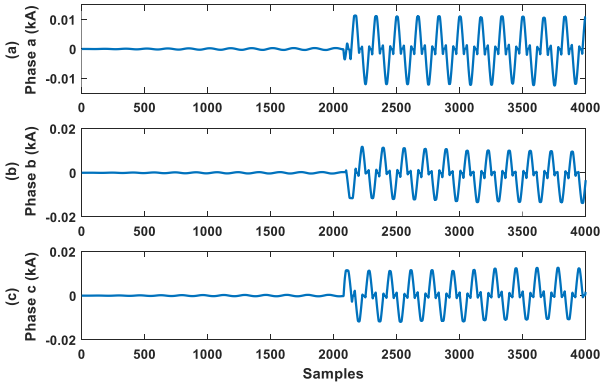

Fig. 11: Sampling data for an external ABCg fault, (a) Phase A, (b) Phase B, (c) Phase C.

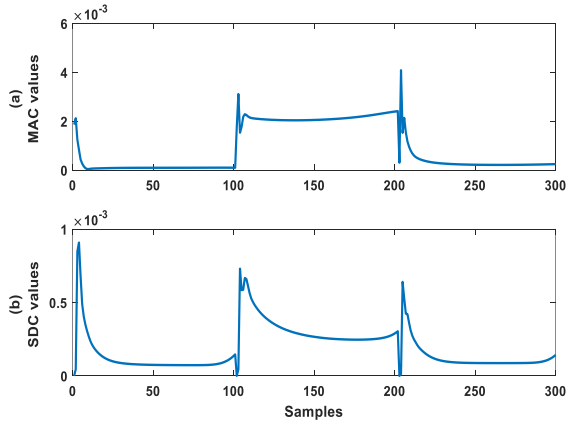

Fig. 12: ST outputs for the three phases for the three-phase external fault, (a) MAC, (b) SDC.

Fig. 11 shows the three-phase current signals for an external fault. Here, the fault impedance is 5 Ohms and the voltage angle of phase A is 120 degrees at the fault inception time.

Fig. 3 shows a single-phase-to-ground internal fault. As can be seen in Fig. 4, there is only one peak in its related MAC, and according to its related SDC, the area under this curve has a relatively higher value than the respective curve of the inrush current. Fig. 5 shows the sampling data of a double-phase-to-ground fault. Fig. 6 indicates that there are two peaks in the MAC of the double-phase-to-ground fault and the area under the SDC for this type of fault is significant. Fig. 7 shows the sampling data for an internal three-phase-to-ground fault. There are three peaks in its MAC and its SDC has still a significant value. According to Figs. 3 to 8, this is obvious that the number of peaks in MAC has a direct relationship with the number of faulted phases.

Fig. 10 shows that for the inrush current signal, there are three peaks in the related MAC, which is the first difference between the output curves of the magnetizing inrush currents and single- and double-phase internal faults. When a double-phase or a three-phase external fault occurs in a power system, transformer differential relay will detect an over-current. Fig. 11 shows the three-phase signals related to a three-phase external fault and its MAC and SDC are shown in Fig. 12. The internal fault has a random nature and its SDC is expected to have a significant value in all frequency samples. So, the area under the SDC for the internal fault is higher than that of the inrush current. In fact, having a significant value in all frequencies of the SDC related to an internal fault is because of the fault-generated high-frequency components. However, for high impedance internal faults, the area under the SDC has a relatively lower value compared to that of the low impedance faults. But, because of existing the high-frequency components, this parameter has still a relatively higher value than that of the inrush currents. As can be seen in Figs. 3-12, the number of peaks in the three-phase MAC and the area under the SDC are the key features to discriminate between the magnetizing inrush currents, internal faults and external faults. To discriminate between the grounded and ungrounded faults, the zero sequence of the three-phase signals should be calculated. This parameter can also make the whole method more precise.

To have a fast, accurate, and easy method, it is necessary to extract some numerical indices from the previous wave type features. Automatic decision-making by numerical parameters is much easier than decision-making by waveforms. So, in this paper, we extract three numerical indices, named C_1, C_2, and C_3 from SDC and MAC of each signal.

C_1: This index represents the number of peaks in the main frequencies of the three phases in the three-phase MAC. If there is a single-phase-to-ground fault, then only one of the main frequencies has a significant value, so there is only one peak in the three-phase MAC and as a result, C_1 would be 1. If there is a double-phase fault, then two of the main frequencies have a significant value, so there are two peaks in its three-phase MAC and as a result, C_1 would be 2. A similar rule exists for a three-phase fault. In the case of having the magnetizing inrush current, all the three main frequencies have a significant value, so there are three peaks in the related MAC and as a result, $C_1 = 3$ for the signal of magnetizing inrush current. For example, in Fig. 6, $C_1 = 2$ and in Fig. 10, $C_1 = 3$.

C_2: This index is the area under the SDC of the signal. As can be seen in Figs. 6 and 10, the area under the SDC of the internal fault is greater than that for the inrush current. So, C_2 can be considered as a discriminative parameter.

C_3: This index is defined to know if the signal is connected to the ground or not. This index is useful for the fault type identification. This is related to the content of the zero sequence of the input signal. To calculate this index, first, by the summation of the samples of the three phases, the zero-sequence current is calculated. Then, ST is applied to the zero-sequence current. C_3 is the maximum value in the MAC of the zero-sequence current. We know that for an ungrounded fault, the zero sequence of a three-phase input signal is nearly zero and for a grounded fault, this parameter has a significant value.

By analyzing a large number of magnetizing inrush, internal and external fault current signals, possible values for C_1, C_2, and C_3 are calculated. Table 1 shows the values of the indices for each fault type.

4.2. Signal Classification

Up to this step, values for each numerical feature are extracted. Now, it is needed to have an efficient classifier to classify the input signals. Fuzzy logic is a good decision-maker and can be used to classify signals according to the numerical features extracted from the input signal. We need a deterministic output as the magnetizing inrush, external fault, single-phase internal fault, double-phase internal fault, double-phase-to-ground internal fault, three-phase internal fault, and three-phase-to-ground internal fault. As a result, a Sugeno-type fuzzy system is required. Digits 1 to 7 represent the signal types mentioned above, respectively. Figs. 13 to 15 show the membership functions for the three variables. These variables are defined according to C_1, C_2, and C_3.

Table 1: Possible values of indices for each signal type.

Disturbance type	C_1	C_2	C_3
Single-phase-to-ground fault	1	0.0032~0.0331	0.0042~0.0229
Double-phase-to-ground fault	2	0.0736~0.2288	0.0021~0.0124
Double-phase fault	2	0.0486~0.1934	4.18×10^{-8}~8.5×10^{-7}
Three-phase-to-ground fault	3	0.2531~0.2626	2×10^{-6}~9×10^{-5}
Three-phase fault	3	0.2018~0.2094	3.9×10^{-8}~5.6×10^{-7}
External fault	3	0.0029~0.0045	3.87×10^{-12}~14×10^{-11}

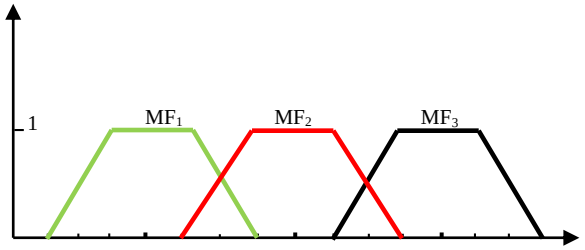

Fig. 13: Membership functions for the variable related to C_1.

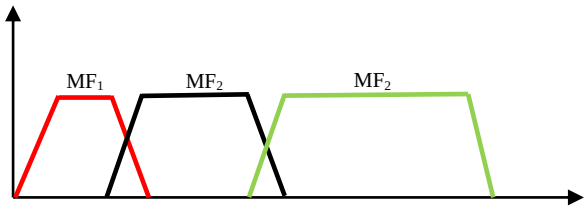

Fig. 14: Membership functions for the variable related to C_2.

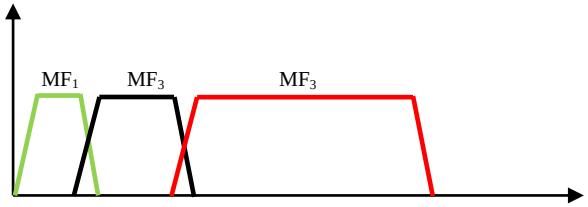

Fig. 15: Membership functions for the variable related to C_3.

Table 2: Values of membership functions for each variable.

Variable	MF_1	MF_2	MF_3
First	0.25-0.75-1.25-1.75	1.25-1.75-2.25-2.75	2.25-2.75-3.25-3.75
Second	0-0.0029-0.0045-0.0046	0.0045-0.0046-0.0321-0.0322	0.0313-0.0314-0.263-0.27
Third	$0\text{-}10^{-12}\text{-}3\times10^{-12}\text{-}10^{-9}$	$10^{-8}\text{-}3\times10^{-8}\text{-}9\times10^{-7}\text{-}10^{-6}$	$10^{-6}\text{-}2\times10^{-6}\text{-}0.023\text{-}0.024$

After defining the membership function, some rules should be defined for the fuzzy engine to make the decision-making process possible. Table 3 shows the set of rules used in this paper.

The values for each membership function must be defined according to the values of the numerical features extracted from the input signal to make it possible for the fuzzy system to classify the input signal correctly and accurately. Table 2 shows the proper value for each membership function.

4.3. Faulted Phase Selection

To find the faulted phases, the three-phase-based MAC is utilized in this paper. It is worth mentioning that ST is separately applied to the differential current signals of phases A, B, and C. Then, we put the extracted MACs in one matrix and name it the three-phase-based MAC. As stated before, there are three regions in the three-phase-based MAC. The first region is related to phase A (samples 1 to 100 in Fig. 4), the second one is related to phase B (samples 101 to 200 in Fig. 4), and the third one is related to phase C (samples 201 to 300 in Fig. 4). Having a peak at the beginning of each region shows that the respective phase has encountered a fault. For example, consider the MAC shown in Fig. 4. At the beginning of the second region, there is one peak in the mentioned MAC. The second region is related to phase B. Therefore, the fault is concluded to be a Bg one. Consider the MAC shown in Fig. 6. In this curve, there are two peaks at the beginning of the first and the third regions. The first region is related to phase A and the third one is related to phase C. Therefore, the faulted phases are concluded to be phases A and C. The flowchart of the proposed algorithm is depicted in Fig. 16.

5. Simulation And Results

A simulation study was done on a system comprising a typical 500 MVA with a 400/230-kV three-phase transformer

Table 3: Decision-making rules.

Rules	Membership function			Output	Result
	Variable 1	Variable 2	Variable 3		
Rule1	MF_3	MF_1	MF_1	MF_1	Inrush
Rule2	MF_1	MF_2	MF_3	MF_2	Single-phase fault
Rule3	MF_2	MF_3	MF_2	MF_3	Double-phase fault
Rule4	MF_2	MF_3	MF_3	MF_4	Double-phase-to-ground
Rule5	MF_3	MF_3	MF_2	MF_5	Three-phase fault
Rule6	MF_3	MF_3	MF_3	MF_6	Three-phase-to-ground
Rule7	MF_2	MF_2	--	MF_7	External fault
Rule8	MF_3	MF_2	--	MF_8	External fault

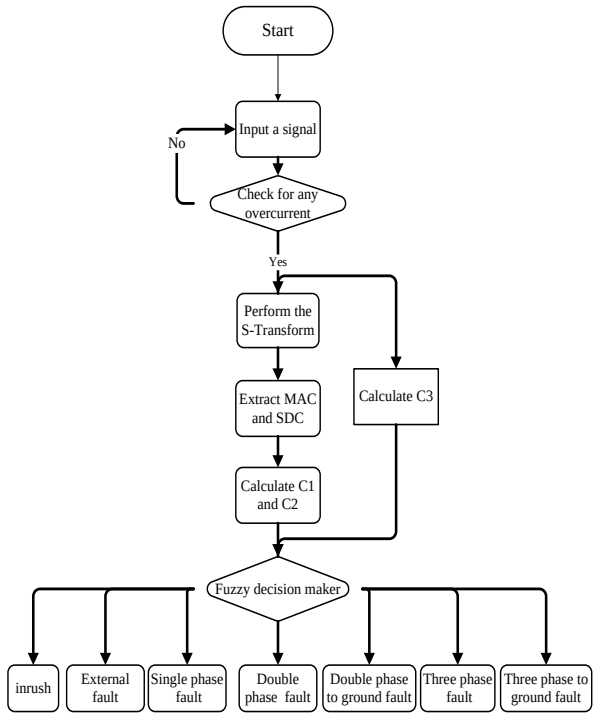

Fig. 16: The flowchart of the proposed method.

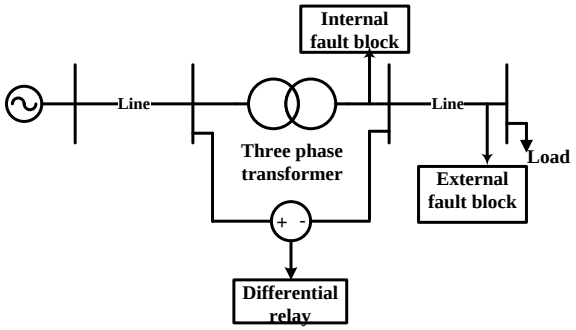

Fig. 17: A single-line diagram of the simulated power system.

that is modeled in PSCAD/EMTDC. To take the effect of long lines into consideration, the distributed model for lines is used in this paper. A single-line diagram of the simulated Y/Δ transformer along with other network elements is shown in Fig. 17.

5.1. Testing the accuracy of the algorithm

To test the performance of the proposed algorithm, 100 signals for each disturbance type are first generated in PSCAD/EMTDC and are classified by the algorithm. To generate different internal faults, the fault type, the fault impedance and the fault inception angle are changed. The source impedance and the voltage angle at the instant of switching are changed to generate different inrush current signals. The results are shown in Table 4.

According to Table 4, it can be seen that this method has a high classification accuracy. The only errors that can be seen in Table 4 are the inrush current and the single-phase fault. There were four mistaken inrush current signals. The output for two of these mistaken signals was "2", which is the index related to the single-phase fault, and the output for two of them was "3", which is the index related to the double-phase fault. For the single-phase-to-ground set of signals, there is one mistaken signal that has the output of "1", which is the index related to the magnetizing inrush currents.

In this paper, faulted phase selection has a very simple algorithm, as described in Section 4.3. This simplicity leads to the high accuracy of this algorithm. This means that all the faulted phases are identified correctly.

5.2. Signal Type Classification

In this section, the process of the signal type classification is analyzed for some sample disturbances. Table 5 shows the related results.

For example, consider the BCg internal fault in Table 5. Here, C_1 is 2, which means that two of the phases have encountered a fault. This means that the signal is an internal or an external fault. The value of C_1 along with the values of C_2 and C_3 shows that there is a double-phase-to-ground internal fault.

5.3. Fault Type Classification and Faulted Phases Selection

To show the robustness of the fault type classification and faulted phases selection algorithm, different internal fault types are generated and tested by the proposed algorithm. Table 6 presents some of the results.

Table 4: The first simulation results for the proposed algorithm.

Disturbance type	Index number	Classification accuracy
Single-phase-to-ground fault	2	99%
Double-phase fault	3	100%
Double-phase-to-ground fault	4	100%
Three-phase fault	5	100%
Three-phase-to-ground fault	6	100%
Inrush current	1	96%
External fault	7	100%

Table 5: The results for the signal type classification.

Applied distrubance	C_1	Index number	C_2	C_3	Fuzzy output	Result
Inrush	3	2	0.0034	2.4×10^{-11}	1	Inrush
Internal fault, Ag	1	3	0.0033	0.0085	2	Single-phase-to-ground fault
Internal fault, BCg	2	4	0.1278	0.0114	4	Double-phase-to-ground fault
Internal fault, ABC	3	5	0.2094	3.9×10^{-8}	5	Three-phase fault
External fault, AB	2	6	0.0059	--	7	External fault
External fault, ABCg	3	1	0.0142	--	7	External fault

Table 6: The results of the fault type classification.

Applied fault	C_1	C_2	C_3	Peak region	Fuzzy output	Result
Bg	1	0.0047	0.0143	2	2	Bg
ACg	2	0.0842	0.0118	1 and 3	4	ACg
AB	2	0.1896	4.3×10^{-8}	1 and 2	3	AB
ABg	2	0.228	0.0057	1 and 2	4	ABg
BC	2	0.1448	1.51×10^{-7}	2 and 3	3	BC
ABC	3	0.2018	5.57×10^{-7}	1, 2 and 3	5	ABC

For example, for the Bg fault in Table 6, the values of C_1, C_2, and C_3 show that there is an internal fault. The value of C_1 shows that only one of the phases has encountered a fault. The second region has a peak and therefore, the test signal is the result of a Bg fault.

5.4. Comparison With Other Algorithms

In [26], an algorithm based on the rate change of the phase angle of the differential current is presented. In [27], using a modified least square algorithm, the sinusoidal part of the differential current is produced, and then using the probabilistic distance measure algorithm, it is analyzed if the signal has resulted from an internal fault or an inrush current. The identification of the single-phase faults is considered in this reference. Another algorithm is presented in [28] to identify only single-phase internal faults. None of these references provide an algorithm for fault type classification and faulted phases selection. The identification of the external faults is not considered in these references either.

References [29] and [30] provide high-frequency-based algorithms for the transformer differential protection. Both fault type classification and external fault identification are not performed in these references.

The algorithm presented in [31] uses the convolutional neural network (CNN) for the transformer differential protection. This type of algorithm needs a large amount of data for the training process, which is a drawback of such protection algorithms. In this reference, different fault types

and external faults are considered in the simulation stage. But there is still no algorithm for fault type identification and faulted phases selection.

The proposed algorithm covers different aspects of the transformer differential protection. The discrimination between the internal faults and inrush currents, fault type classification and faulted phases selection, and the identification of external faults are all considered in the proposed algorithm. Besides, in some references such as [32-34], the existence of the low-order harmonic components affects the performance of the algorithms. The proposed algorithm covers the gap between the fundamental frequency-based algorithms and high-frequency-based algorithms. Low-order harmonic components such as the ones resulting from the CT saturation do not affect the performance of the proposed algorithm.

6. Conclusion

This paper presents a new algorithm to discriminate between the magnetizing inrush currents, external faults, and internal faults. The algorithm uses wave shapes of the three signal types. In the first step, some discriminative features are extracted from the MAC and SDC of the faulted signal using ST. In the second step, to classify the transformer signals according to the numerical indices, a fuzzy expert system is utilized. Converting the wave shape characteristics to the numerical features simplifies the classification process. Using fuzzy logic as a decision-maker, makes the algorithm more flexible and reliable. Finally, testing the proposed algorithm by means of the test signals generated by PSCAD/EMTDC software shows the effectiveness of the proposed method in the transformer differential protection.

Credit Authorship Contribution Statement

Saeid Hasheminejad: Conceptualization, Data curation, Formal analysis, Funding acquisition, Investigation, Methodology, Project administration, Resources, Software, Supervision, Validation, Visualization, Roles/Writing - original draft, Writing - review & editing.

Declaration Of Competing Interest

The authors declare that they have no known competing financial interests or personal relationships that could have appeared to influence the work reported in this paper. The ethical issues; including plagiarism, informed consent, misconduct, data fabrication and/or falsification, double publication and/or submission, redundancy has been completely observed by the authors.

References

[1] H. Esponda, E. Vazquez, M. A. Andrade, and B. K. Johnson, "A setting-free differential protection for power transformers based on second central moment", *IEEE Transactions on Power Delivery*, vol. 34, no. 2, pp.750-759, 2019.

[2] H. Dashti, and M. Sanaye-Pasand, “Power transformer protection using a multi-region adaptive differential relay”, *IEEE Transactions on Power Delivery*, vol. 29, no. 2, pp. 777-785, 2014.

[3] A. Ashrafian, M. Mirsalim, and M. A. S. Masoum, "Application of a recursive phasor estimation method for adaptive fault component based differential protection of power transformers", *IEEE Transactions on Industrial Informatics*, vol. 13, no. 3, pp. 1381-1392, 2017.

[4] M. R. Tripathy, P. Maheshwari, and H. K. Verma, "Power transformer differential protection based on optimal probabilistic neural network", *IEEE Transactions on Power Delivery*, vol. 25, no. 1, pp. 102-112, 2010.

[5] F. Peng, H. Gao, and Y. Liu, "Transformer sympathetic inrush characteristics and identification based on substation-area information", *IEEE Transactions on Power Delivery*, vol. 33, no. 1, pp. 218-228, 2018.

[6] M. Tripathy, R. P. Maheshwari, and H. K. Verma, "Advances in transform protection: A review", *Electric Power Components and Systems*, vol. 33, no. 11, pp. 1203-1209, 2005.

[7] A. G. Phadke, and J. S. Thorp, "A new computer-based flux-restrained current differential relay for power transformer protection", *IEEE Transactions on Power Apparatus and Systems*, vol. 102, no. 11, pp. 3624-3629, 1983.

[8] T. Zheng, T. Huang, Y. Ma, Y. Z. Zhang, and L. Liu, " Histogram-based method to avoid mal-operation of transformer differential protection due to current-transformer saturation under external faults", *IEEE Transactions on Power Delivery*, vol. 33, no. 2, pp. 610-619, 2018.

[9] M. C. Shin, C. W. Park, and J. H. Kim, "Fuzzy logic based relaying for large power transformer protection", *IEEE Transactions on Power Delivery*, vol. 18, no. 3, pp. 718-724, 2003.

[10] S. K. Murugan, S. P. Simon, K. Sundareswaran, P. S. R. Nayak, and N. P. Padhy, "An empirical Fourier transform-based power transformer differential protection", *IEEE Transactions on Power Delivery*, vol. 32, no. 1, pp. 209-218, 2017.

[11] P. B. Thote, M. B. Daigavane, P. M. Daigavane, and S. P. Gawande, "An intelligent hybrid approach using KNN-GA to enhance the performance of digital protection transformer scheme", *Canadian Journal of Electrical and Computer Engineering*, vol. 40, no. 3, pp. 151-161, 2017.

[12] A. R. Moradi, E. Ebadian, M. Yazdani-Asrami, and M. Taghipour,"Artificial intelligence based techniques for distinguishing inrush current from faults in large power transformers", *International Review of Electrical Engineering*, vol. 6, no. 5, pp. 2198-2206, 2011.

[13] R. P. Medeiros, and F. B. Costa, "A wavelet-based transformer differential protection with differential current transformer saturation and cross-country fault detection", *IEEE Transactions on Power Delivery*, vol. 33, no. 2, pp. 789-799, 2018.

[14] R. P. Medeiros, and F. B. Costa, "A wavelet-based transformer differential protection: internal fault

detection during inrush conditions", *IEEE Transactions on Power Delivery*, vol. 33, no. 6, pp. 2965-2977, 2018.

[15] F. Zhao, and R. Yang, " Power Quality Disturbance Recognition Using S-transform", *IEEE Transaction on power delivery*, vol.25, no. 4, pp. 944-950, 2007.

[16] A. Hooshyar, S. Afsharnia, M. Sanaye-Pasand, and B. M. Ebrahimi, "A new algorithm to identify magnetizing inrush conditions based on instantaneous frequency of differential power signal", *IEEE Transactions on Power Delivery*, vol. 25, no. 4, pp. 2223-2233, 2010.

[17] D. Barbosa, U. C. Netto, D. V. Coury, and M. Oleskovicz, "Power transformer differential protection based on Clark's transform and fuzzy system", *IEEE Transactions on Power Delivery*, vol. 26, no. 2, pp. 1212-1220, 2011.

[18] S. A. Saleh, and M. A. Rahman, "Testing of a Wavelet-Packet-Transform-Based Differential Protection for Resistance-Grounded Three-Phase Transformers", *IEEE Transactions on Industrial Applications*, vol. 46, no. 3, pp. 1109-1117, 2010.

[19] S. A. Saleh, B. Scaplen, and M. A. Rahman, "A new implementation method of wavelet-pocket-transform differential protection for power transformers", *IEEE Transactions on Industrial Applications*, vol. 47, no. 2, pp. 1003-1012, 2011.

[20] F. Naseri, Z. Kazemi, M. M. Arefi, and E. Farjah, "Fast discrimination of transformer magnetizing current from internal faults: An extended Kalman Filter-Based Approach", *IEEE Transactions on Power Delivery*, vol. 33, no. 1, pp. 110-118, 2018.

[21] S. Hasheminejad, S. Esmaeili, and S. Jazebi, "Power quality disturbance classification using S-Transform and hidden Markov model", *Electric Power Components and Systems*, vol. 40, no. 10, pp. 1160-1182,2010.

[22] H. W. Dommel, "Transformer models in the simulation of electromagnetic transients", *Proceedings of 5TH power system computing conference*, 1975, paper 3.1/4

[23] D. Woodford, "Introduction to PSCAD/EMTDC V3", *Manitoba HVDC research center Inc*, 2000.

[24] S. Jazebi, B. Vahidi, and S. H. Hosseinian, "A novel discriminative approach based on Hidden Markov Models and wavelet transform to transformer protection", *Journal of Simulation*, vol. 86, no. 2, pp. 93-107, 2010.

[25] R. G. Stockwell, L. Mansinha, and R. P. Lowe, "Localization of the complex spectrum: The S-transform", *IEEE Transactions on signal processing*, vol. 44, no. 4, pp. 998-1001, 1996.

[26] H. Samet, M. Shadaei, and M. Tajdinian, "Statistical discrimination index founded on rate of change of phase angle for immunization of transformer differential protection against inrush current", *Int. j. of Elect. power and ener. Syst*., vol.13, no. 4, 107381, 2022.

[27] M. Tajdinian, and H. Samet, "Application of probabilistic distance measures for inrush and internal fault currents discrimination in power transformer differential protection", *Elect. Power Syst. Res*, vol. 19, no. 3, 107012, 2021.

[28] A. Moradi, and S. M. Madani, "Predictive formulas to improve transformer protection during inrush current using the proposed equivalent circuit", *IEEE trans. on power deliv*, vol. 35, no. 2, pp. 919-928, 2020.

[29] L. D. Simoes, H. J. D. Costa, M. O. Aires, R. P. Medeiros, F. B. Costa, and A. S. Bretas, "A power transformer differential protection based on support vector machine and wavelet transform", *Elec. power syst. Res*., vol. 19, no. 7, 107297, 2021.

[30] M. N. O. Aires, R. P. Medeiros, K. M. Silva, J. J. Chavez, and M. Popov, "A wavelet-based restricted earth-fault power transformer differential protection", *Elect. Power syst. Res*., vol. 19, no. 6, 107246, 2021.

[31] S. Afrasiabi, M. Afrasiabi, B. Paarang, and M. Mohammadi, "Integration of accelerated deep neural network into power transformer differential protection", *IEEE trans. on indist. Inform*., vol. 16, no. 2, pp. 865-876, 2020.

[32] H. Weng, S. Wang, X. Lin, Z. Li, and J. Huang, " A novel criterion applicable to transformer differential protection based on waveform sinusoidal similarity identification", *Int. J. Electr. Power Energy Syst*., vol. 10, no. 5, pp. 305-314, 2019.

[33] L. Zhang, Q. Wu, and T. Ji, "Identification of inrush currents in power transformers based on high-order statistics", *Electr. Powe Syst. Res*., vol. 14, no. 6, pp. 161-169, 2017.

[34] F. Naseri, H. Samet, T. Ghanbari, and E. farjah, " Power transformer differential protection based on least square algorithm with extended kernel", *IET science, Measur. Techn*., vol. 18, no. 8, pp. 1102-1110, 2019.

BIOGRAPHY

Saeid Hasheminejad was born in Kerman, Iran in 1985. He received his B.Sc., M.Sc., and Ph.D. degrees in 2008, 2011, and 2016, respectively. He is currently an assistant professor at the Graduate University of Advanced Technology, Kerman, Iran. His research interests are in the areas of signal processing, power quality, and power system protection.